1-1-1975

Stress distribution in a curved plate girder bridge.

John M. Talhelm

STRESS DISTRIBUTION IN A CURVED PLATE GIRDER BRIDGE

by

John M. Talhelm

A Thesis

Presented to the Graduate Committee

of Lehigh University

in Candidacy for the Degree of

Master of Science

in

Civil Engineering

May 1975

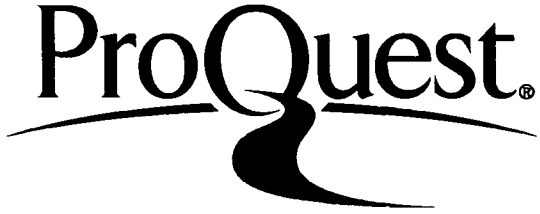

This thesis is accepted and approved in partial fulfillment of the requirements for the degree of Master of Science.

May 9, 1975
(date)

Prof. Ben T. Yen

Prof. D.A. VanHorn
Chairman
Department of Civil Engineering

TABLE OF CONTENTS

LIST OF TABLES

LIST OF FIGURES

ABSTRACT

Strain and deflection measurements were taken at several structural steel details on a curved, steel plate girder bridge. Strain gages were mounted over the depth of the webs on both the inside and outside girders as well as across the flange widths to measure the strains caused by static and dynamic loads. An HS 20-44 truck load of AASHTO was simulated through the use of a FHWA's test vehicle. Analog trace recordings were taken during the testing. For comparison, static live load stresses at the gage locations were estimated by using the computer program CURVBRG.

Computed and measured static and dynamic live load stresses compared well. The measured values were generally lower. Stresses in a girder were higher when the truck was in a position near the girder. Maximum stresses occurred in the inside girder when the truck was at the centerline of the span. Both the measured and computed stresses, however, were lower than the design stresses. Measured deflections were also consistant with the computed values but again were lower.

Impact factors were evaluated as the ratio of stresses or deflections during a truck run to those during a crawl run of the truck over the bridge. These factors were in all but two cases lower than those computed using the impact formula of AASHTO for straight girders. Comparison of measured live load stresses with the allow-

able fatigue strength for highway bridge details, on the other hand, suggests that the bridge would not encounter problems of fatigue after it is open to traffic.

1. INTRODUCTION

1.1 Background and Objectives

In recent years highway engineers and designers have been faced with a relentless trend of increasing costs for both labor and materials and decreasing amounts of available land. Prompted by this situation the use of plate or box girders, curved in the horizontal plane has become more popular. These girders enable the designer increased structural efficiency while economizing on space and substructure construction. Also the curved shape presents an appealing, esthetic view to the general public.

Curved steel plate or box girders are primarily used in the construction of elevated entrance and exit ramps for multi-lane highway systems. These curved girders usually interact with the concrete deck to form integral structural members in resisting the forces of a vehicle and the weight of the member itself.

However due to the bending and torsional characteristics inherent in curved members, the analysis and design of these structures have been open to many uncertainties. As a result, extensive research has been conducted by such men as Culver and Mozer in the area of stability and by Armstrong and Greig through field testing of existing curved girder bridges. [1,2,3]

Numerous in-depth studies resulting from the work of the Consortium of University Research Teams (CURT) have been initiated at

several universities in the area of curved girders. One such project currently under way at Lehigh University is to study the fatigue strength of curved steel bridge elements. As with CURT, this project is conducting theoretical and experimental studies in the laboratory as well as testing curved steel girder bridges in the field. The field testing of a curved girder bridge ramp of the Bridgeport bridge (S-9896) between Norristown and Bridgeport, Pennsylvania is the subject of this report.

The Bridgeport bridge ramp was subjected to stationary as well as travelling truck loads during testing. The primary thrust of the testing will be a correlation between the measured stresses, and analytical stresses obtained from an available computer program (CURVBRG).[4] Secondly the stress measurements acquired during field testing will be compared with laboratory data to predict the performance, with respect to fatigue, of the bridge ramp when open to traffic.

1.2 Description of the Bridge

The Bridgeport curved steel girder bridge ramp was constructed in 1974 and was not open to traffic at the time of testing. The structure, as indicated in figure 1, is a three span, steel, curved deck, girder bridge. Design was by the 1969 A.A.S.H.O. Standard Specifications for Highway Bridges and the 1970 Interim Specifications. All references to the structure will be confined to the center span where the instrumentation was applied.

Figure 2 is a plan view of the center span. The span has a centerline radius of curvature of 296.44 ft. and a centerline span length of 125.65 ft. Transverse floor beams are spaced equally at 7.85 ft. along the centerline.

An elevation of the main longitudinal girders is depicted in figure 3. These two girders are welded plate girders with flanges of different area along the span. ASTM A-572, Grade 50 steel was used for plates in excess of 1½ inches. Full depth intermediate stiffeners are also shown throughout the length of the girders.

A typical cross sectional view of the bridge is presented in figure 4. As shown, the transverse bracing is comprised of W33X130 rolled sections of ASTM A-36 steel. The composite deck consists of permanent metal decking covered by a 9 inch, 3000 psi., reinforced concrete slab.

The center span support is fixed and radial over pier 1 and simply supported and on a skew of approximately 22.5° over pier 2. Figure 5a and 5b show the typical support conditions at these locations. The bearing plate is bronze, ASTM B-22, Alloy B, while the sole and masonry plates are ASTM A-588 steel. The spherical surface of the bearing plates is self-lubricated and allows for rotational movements inherent with curved steel girders.

2. FIELD TESTING

2.1 Strain Recording System

2.1.1 Strain Gages

Eighty electrical resistance strain gages and four deflectometers were mounted on the center span of the bridge. The strain gages were placed near structural details at the webs and flanges of the girders (figure 6). Also, one transverse beam diaphragm was instrumented. Figure 7 indicates the locations of the deflectometers which were made by the Federal Highway Administration (FHWA) and placed at the center line and a quarter point of the girders. The exact locations of the gages are depicted in Figures 8 through 14.

The gages used were ¼ in. long electrical resistance gages of the foil type. Moisture and other environmental effects to the gages were prevented by application of weather proof coatings. (5) To minimize the effect of temperature changes, the gages were connected to temperature compensating gages and plates.

The FHWA deflectometer consists of a triangular aluminum plate 1/8 in. thick with four SR-4, A-3 strain gages located at the base. (3) The deflectometers were clamped to the edges of the bottom flanges of the girders. Through the use of a taut steel wire anchored to the ground and initiating a deflection of the aluminum plate

greater than the expected deflection of the girder, the deflection of the bridge, under load, was measured.

2.1.2 Recording Equipment

For recording the strain readings the FHWA's instrument van was utilized. The equipment includes a set of amplifiers, ultraviolet analog trace recorders, an analog-to-digital converter, and an FM digital tape recorder. A total of 64 gages were monitored simultaneously. Prior to the test the zero reading of each gage was recorded and periodic checks of this zero level were conducted to reduce drifting during monitoring. All data was stored on a 9-track magnetic tape simultaneously with the analog trace recorder. The latter yielded a trace of the live load strain magnitudes as a function of time.

Figure 15 shows a plan view depicting the deck instrumentation for the dynamic (travelling truck) tests. The two pheumatic striker hoses were positioned over the bridge supports. These hoses provided a longitudinal position indicator of the truck load on each oscillograph and tape record. Two additional hoses were placed 50 ft. from each end of the center span to monitor vehicle speed and to activate the oscillographs.

2.2 Test Loading

Loading was provided by the FHWA's test truck simulating a standard AASHTO HS-20-44 load scheme. Figure 16 shows a comparison between the actual loading of the test truck versus the prescribed loading of AASHTO. [6] The total weight of the test truck was 78.38 kips as opposed to the AASHTO load of 72 kips. Distribution of the weight to the axles is also shown in Figure 16.

Static as well as dynamic live load testing was conducted. In the static tests the truck was positioned at four different positions as shown in figures 17a and 17b. The truck was positioned over the centerline and over the quarter points of the span. The centerline of the truck was 7 ft. 3 in. from the curb on girder 2(G2) and 5 ft. 3 in. from the curb on girder 1(G1) (figure 15). Strain variations were recorded with the truck in position and with the truck off the load position.

The dynamic loading consisted of both crawl and speed runs with the truck traversing the bridge in three lanes in both the north and south direction. The lanes were located along the inside and outside curbs as well as along the longitudinal centerline of the bridge (figure 15). Table 1 summarizes this information.

3. STRESS AND DEFLECTION EVALUATION

3.1 Measured Stresses

The strain readings accumulated during the field test of the Bridgeport bridge were stored on magnetic tape as well as analog trace recordings. The magnetic tapes were to be used by the FHWA in evaluating the performance of the recording and conversion systems. For this paper the measured strains were extracted from the analog trace recordings through a reduction formula developed by the FHWA:

$$\varepsilon = \frac{GR(1.0 + 0.000415L)\ (TD)\ \left(\frac{C.Gain}{O.Gain}\right)}{GF\ (6.04 \times 10^{5})\ (CD)} \qquad \text{(Eqn. 1)}$$

where:

GR = gauge resistance

L = length of cable in feet

TD = trace deflection in inches or a reading in volts from a visible dial

C.Gain = calibration gain

O.Gain = operator gain

GF = gauge factor

CD = calibration deflection in inches on the trace reading or volts on the dial, making sure to use only the positive value.

After the strains were calculated the measured stresses were obtained by applying the Young's modulus, $\sigma = \varepsilon E$.

All stresses for the static and dynamic live load cases were calculated in this manner.

3.2 Computed Stresses

In conjunction with the measured values, stresses at the gage locations were calculated by using the CURVBRG program. This Program was developed for analyzing stresses and deflections of curved open girder bridges.[4] It idealizes the bridge superstructure as a two dimensional grid considering five types of components: girders, slab strips, beam type diaphragms, diagonally braced cross frames and wind bracing members. For the Bridgeport model the first three types were utilized.

The input data to the program is in standard FORTRAN format. Other features include automatic generation of grid joints to include coordinates, definition of girder properties in cross section dimensions and automatic generation of the data for slab strips and diaphragms.

A cross section of the CURVBRG model of the Bridgeport bridge is depicted in figure 18. The cross section was considered as a composite deck with the curbing neglected. Also, because of the program's limitations, it was not possible to include the knee bracing at the beam diaphragms. The absence of these structural components in the model decreased the overall stiffness of the structure

and was the probable cause for slightly higher computed stresses. Since the bridge is composite in nature the input data for CURVBRG called for the effective width of the slab. The effective width was determined by AASHTO specification 1.7.00 for a beam with an overhang and was equal to twelve times the least thickness of the slab.[6]

In order to model the four static loading cases it was necessary to distribute the loads, first to the transverse floor beams and then to the main girders. Distribution of these loads was carried out according to AASHTO specifications 1.3.1 (B) and (C).[6] Figure 19 shows schematically the distribution sequence for one load case. This sequence was repeated for the other three load cases. Distribution in both directions was over simple supports.

With the input of data, stresses were calculated for the static live load tests. CURVBRG does not possess the capability for dynamic loading and no dynamic stresses were calculated for the speed runs for this report.

3.3 Deflections

From the measured strains in the strain gages of the deflections of the girder flanges were calculated using the formula:

$$\Delta = \frac{\dot{\varepsilon}\ (1.0 + 0.0065\ell)\ \Delta_f}{4.0} \qquad \text{(Eqn. 2)}$$

where:

ε = strain computed from Eqn. 1

ℓ = length of the deflection gage wire

Δ_f = deflection factor for a specific gage calibrated by FHWA

Deflections at the points of the deflectometers were also computed by using the CURVBRG computer program. The comparisons of measured and computed deflections as well as measured and computed stresses are made in the next chapter.

4. CORRELATION OF RESULTS

4.1 Static Stresses

The static live load stresses on the Bridgeport bridge ramp showed good agreement between the measured stresses and those estimated analytically through the CURVBRG program. The maximum stresses in a girder occurred when the test truck was positioned near the girder.

Figures 20 through 26 depict the stress distribution in the instrumented cross-sections of the curved girder for load case 4 (Fig. 18). With the test truck positioned over the centerline of the span close to the inside girder (G2), maximum stresses in the bridge were produced at the inside girder. For this loading position as well as the other three, the computed stresses agreed more favorably with the measured stresses in the web than in the flanges and in practically all cases the computed values were higher. This is probably due partially to the omission of the curbing and the knee brace plates in the analysis and partly to the nature of the computer program.[4]

The maximum static live load stresses in all cross sections are listed in Table 2 together with the design stresses. Both the computed and measured stress are lower than the design stresses being about one-third to two-thirds of the design values.

The measured stresses at the beam diaphragm were very low for all four static loading cases. The magnitudes were always below 0.5 ksi. This implies that there was little interaction between the girders transmitted through the beam diaphragm. There was no axle or wheel loads on the deck directly over the diaphragms to examine the stress magnitudes. However, the stresses for that particular loading position would be more related to direct bearing on the deck and transmission, rather to the interaction of the curved girders.

4.2 Dynamic Stresses

The test vehicle made crawl and speed runs in the three test lanes in both the northbound and the southbound directions (Table 1). The bridge ramp is intended for northbound traffic. Since there were only minor differences in stress magnitudes for the two directions of truck runs the discussion or dynamic effects is made on the northbound run results.

Figure 27 shows an example of the ultraviolet analog trace record from which the measured stresses were reduced according to Eq. (1). The traces were recorded during a speed run of the test truck. The general rise and return of any trace line correspond to the static live load strain response of a gage due to the approaching and leaving of the truck. The small-amplitude but frequent zig-zag fluctuations of the trace lines indicate the dynamic or impact effects of the truck run. The highest point of a trace is a measure

of the maximum live load plus impact stress at that gage. The impact effect depended not only on the position and maximum speed of the truck but also very much on the oscillation of the truck as it came onto the bridge and on the vibrational characteristics of the bridge structure.

Table 3 summarizes the impact factors for the different loading conditions when the truck was at three test lanes and traveling at four different speeds. Impact factor is defined as the difference between the speed run and crawl run stresses divided by the crawl run stress. It is obvious from the table that the impact factors based on stresses did not increase as the speed of the truck was increased. For comparison, the impact factors computed using the AASHTO formula for straight girders are also listed in the table. None of the measured factors were higher than the value by the formula.

As in the case of static loading, the dynamic stresses in a girder were higher when the truck is near to the girder, and the maximum dynamic (live load plus impact) stresses occurred in the inside girder (G2). Table 4 lists the design and measured maximum live load plus impact stresses at all the gaged sections of the Bridgeport ramp bridge. Also given are the ratios of the two values. In all cases the design values were higher. However, it should be noted that the design stresses were at the edges of flanges whereas the measured values were at a distance of 2 in. from the edge. Adjust-

ment of the design stresses to the gage locations results in slightly lower (15%) values for the stress ratios but in general the measured stresses are still lower.

The maximum dynamic stress in the instrumental beam diaphragm was about 1.5 ksi.

4.3 Deflections

The measured static deflections at the bottom of the girders could be compared with values from the CURVBRG computer program. Table 5 gives the truck position and the corresponding deflection values in the girders by measurement and by computation. The agreement is quite satisfactory. Also in agreement with the comparison of stresses, the measured deflections were in general lower than the predicted, and the deflections were higher at a girder when the truck was in a lane near by.

No computed dynamic deflections were obtained to correlate with the test results. The maximum recorded dynamic deflection was 0.361 in. on the inside girder. By comparing the crawl run and speed run deflections, impact factors have been computed analogous to those determined from stresses and are listed in Table 6. Again, for stresses, the impact factors did not increase with increasing speed of the truck. The maximum value was 26.4% of the live load deflection. In comparing the test values with those computed from the AASHTO formula for straight girders, it was found that in one loading

case the test impact factor was higher (26.4 versus 19.9%). A similar situation existed for those loading cases when the truck was southbound. It appears that, if an impact factor is to be used for design and fatigue strength evaluation, additional studies need to be made in this area.

4.4 Prediction of Performance in Fatigue

The maximum dynamic (live load plus impact) stresses in the flanges are also the maximum stress ranges to which the flanges were subjected. Table 4 listed the measured stress ranges at the gages. The extrapolated stress ranges at the edges of the flanges were approximately 15% higher with the highest maximum stress range about 5.5 ksi. at sections H and J (Figs. 6, 11 and 12). The corresponding AASHTO fatigue strength category for these locations is category C with an allowable stress of 12 ksi for over two million cycles.[8] Consequently, there appears to be a low probability that the bridge will develop fatigue cracks under normal traffic conditions.

Of concern to bridge strength evaluation is the possibility of web plate bending stresses due to lateral deflection of the webs when the bridge is under load. The web plate bending stresses as revealed by the back-to-back gages on the girder webs were very low, in the order of 0.5 ksi. This indicates there was little web deflection and little chance of developing fatigue cracks.

5. SUMMARY AND CONCLUSIONS

As stated earlier the overall summation and conclusions derived from the testing of the Bridgeport ramp are confined to traffic traversing the bridge in the northbound direction. This concentration on direction is due to the fact that when opened to traffic the bridge will serve as an entrance ramp only. Also single lane traffic will be initiated and if necessary provision has been made for two lane traffic over the ramp.

The Bridgeport ramp curved girder bridge is primarily for single lane northbound vehicles when open to traffic. In this study, the bridge deck was divided into three test lanes and the test truck travelled in both directions. Little difference was found in the stresses and deflections for the two directions of test truck runs. Therefore, the following summary and conclusions can be drawn regardless of traffic direction:

1. The maximum live load stresses occurred at the inside girder (G2) with the truck travelling close to the curb above this girder (lane 1). These maximums occurred both for the dynamic as well as static truck loading on the bridge. This condition is in agreement with results from similar studies.[2,3]
2. The maximum deflections were also at the inside girder, with the test truck near the girder and at the center of the span.

3. The maximum impact factors also occurred when the truck was near the inside girder. This was true for impact factors computed as stresses or deflections.
4. The maximum magnitude of impact factors based on stresses was higher than the allowable value derived from the AASHTO formula for straight bridges. This suggests that further studies may be needed in this area.
5. The web bending stresses were negligible and there was no "oil canning" action of the webs.
6. The static stresses and deflections of the bridge evaluated through the computer program CURVBRG show good agreement with the measured stresses and deflections.
7. Both the computed (CURVBRG) and measured static live load stresses were lower than the design live load stresses. The measured dynamic (live load plus impact) stresses were always lower than the design values, sometimes by a large percentage.
8. The low live load stresses measured during the test truck loading indicates that there is very low probability of fatigue problems with this structure. The maximum dynamic live load stresses (maximum stress ranges) for the bridge details were far below range for more than 2,000,000 cycles.

Record Number	Lane	Nominal Speed/Dir.	Speed (mph)
1	Cal.	-	-
2	1	C - NB	-
3	1	C - NB	-
4	2	C - NB	-
5	3	C - NB	-
6	1	20 mph - NB	22.26
7	2	20 mph - NB	20.63
8	3	20 mph - NB	22.03
9	2	S - NB	34.44
10	1	20 mph - SB	22.02
11	1	S - NB	33.76
12	3	S - NB	31.34
13	2	20 mph - SB	22.88
14	2	C - NB	-
15	3	20 mph - SB	22.33
16	3	C - NB	1.81
17	1	C - SB	1.70
18	2	C - SB	1.66
19	3	C - SB	1.61
20	1	C - SB	1.69
21	2	C - SB	1.69
22	3	C - SB	1.57
23	1	S - SB	29.65
24	1	10 mph - NB	10.68
25	2	S - SB	32.61
26	2	10 mph - NB	10.85
27	3	S - SB	25.27
28	3	10 mph - NB	10.56
29	2	S - SB	32.64
30	Cal.	-	-

C - Crawl Run
S - Speed Run
NB - Northbound
SB - Southbound

Table 1

Section	Max. Stress (LL,ksi)		
	Design	Measured	CURVBRG
A	5.47	1.77	2.65
B	5.45	3.26	2.70
C	5.38	2.19	2.63
D	4.27	1.20	1.77
E	3.95	-	-
F	5.46	1.80	3.29
G	4.72	-	1.98
H	5.06	2.85	3.20
I	5.00	2.13	3.13
J	4.99	2.82	2.86
K	3.97	2.37	1.35
L	3.75	-	-
M	5.24	-	-
N	4.72	0.69	2.64
O	4.66	-	-

Table 2 - Static Load Stresses

Truck Speed	Lane 1 Max. σ	Lane 1 Max. Crawl σ	Lane 1 I (%)	Lane 2 Max. σ	Lane 2 Max. Crawl σ	Lane 2 I (%)	Lane 3 Max. σ	Lane 3 Max. Crawl σ	Lane 3 I (%)
Crawl	3.97	3.97	-	2.13	2.13	-	2.30	2.30	-
10	4.65		17.1	2.42		13.6	2.44		6.1
20	3.62		-8.8	2.10		-1.4	2.40		4.3
Speed	3.50		-11.8	2.50		17.4	2.48		7.8
AASHTO I Factors			20.0			19.9			19.6

Table 3 - Impact Factors

Section	Max. Stress (LL+I, ksi)		Design / Measured
	Design	Measured	
A	6.53	2.68	2.44
B	6.52	-	-
C	6.42	2.48	2.59
D	5.09	1.78	2.86
E	4.72	-	-
F	6.52	2.27	2.87
G	5.64	1.82	3.09
H	6.03	4.65	1.30
I	5.96	3.31	1.80
J	5.95	4.51	1.31
K	4.74	2.81	1.69
L	4.47	-	-
M	6.25	3.63	1.72
N	5.62	-	-
O	5.56	2.24	2.48

Table 4 - Dynamic Load Stresses

Truck Position	Inside Girder G2		Outside Girder G1	
	Measured	Curvbrg	Measured	CURVBRG
Lane 1	0.308in.	0.353in.	0.031in.	0.105in.
Lane 3	0.06 in.	0.05 in.	0.238in.	0.477in.

Table 5 - Maximum Deflection

Truck Speed	Lane 1 Max. Δ	Lane 1 Max. Crawl Δ	Lane 1 I (%)	Lane 2 Max. Δ	Lane 2 Max. Crawl Δ	Lane 2 I (%)	Lane 3 Max. Δ	Lane 3 Max. Crawl Δ	Lane 3 I (%)
Crawl	0.308	0.308	-	0.201	0.201	-	0.238	0.238	-
10	0.355		15.3	0.201		-	0.269		13.0
20	0.361		17.2	0.214		6.5	0.238		-
Speed	0.321		4.2	0.254		26.4	0.268		12.6
AASHTO I Factors			20.0			19.9			19.6

Table 6 - Impact Factors

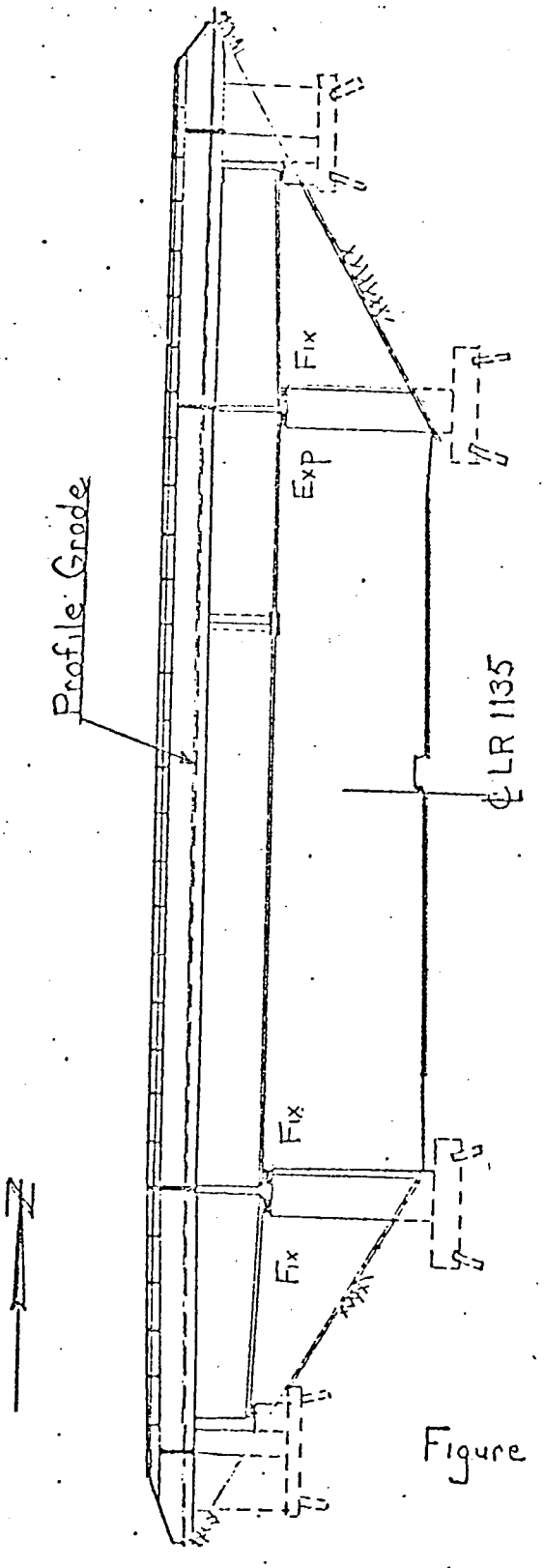

East Elevation

Figure 1

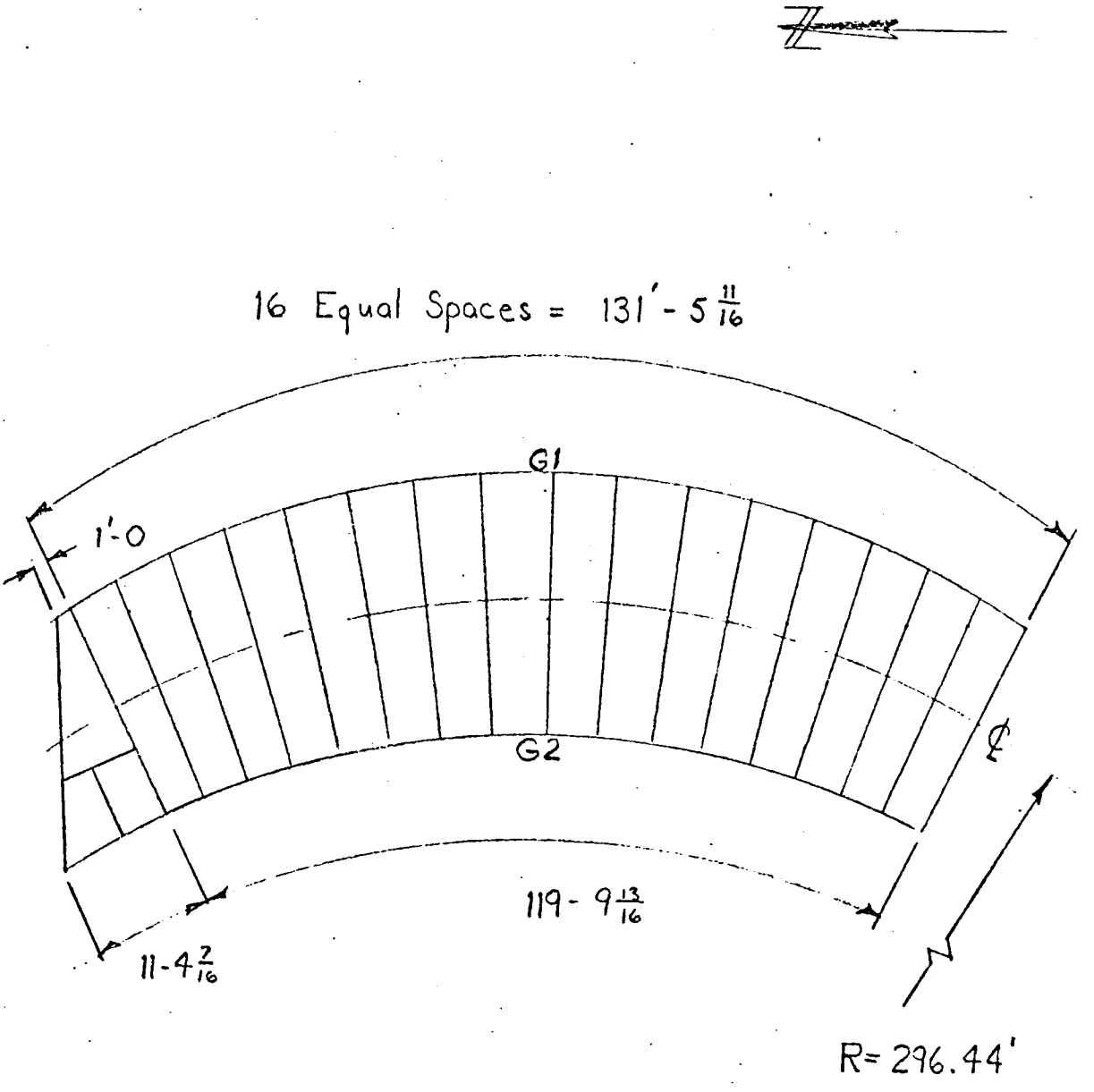

Plan View

Figure 2

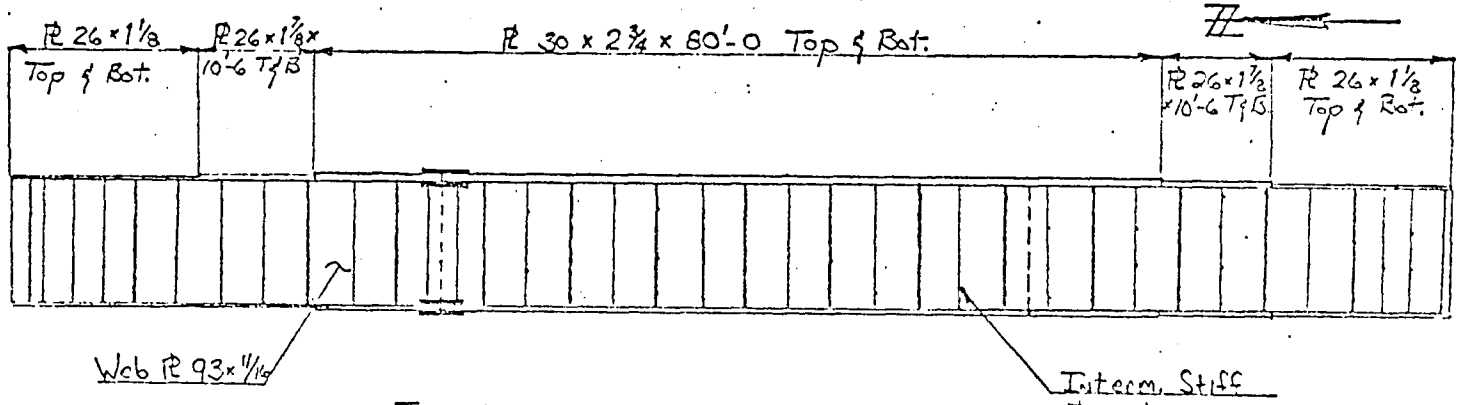

Inside Elevation - Girder G1

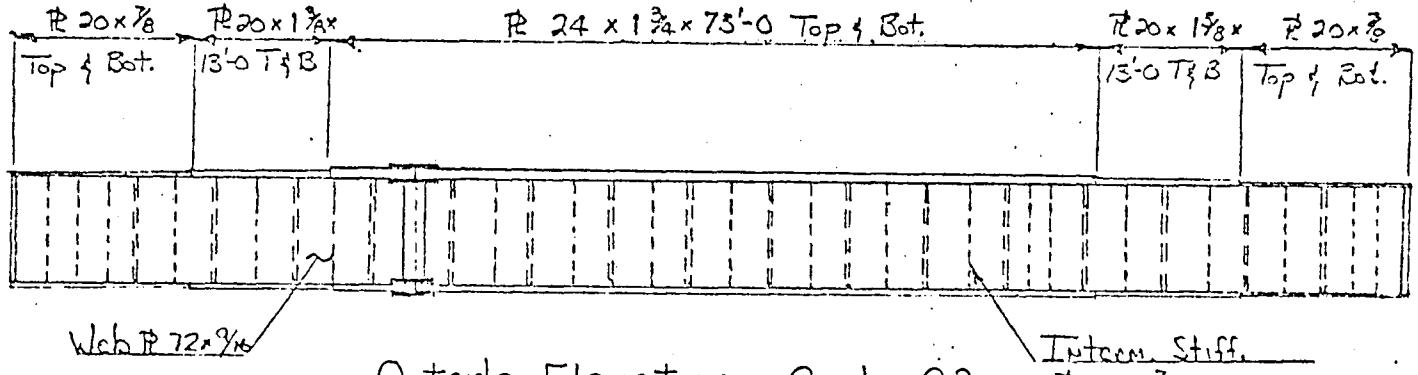

Outside Elevation - Girder G2

Figure 3. Elevation.

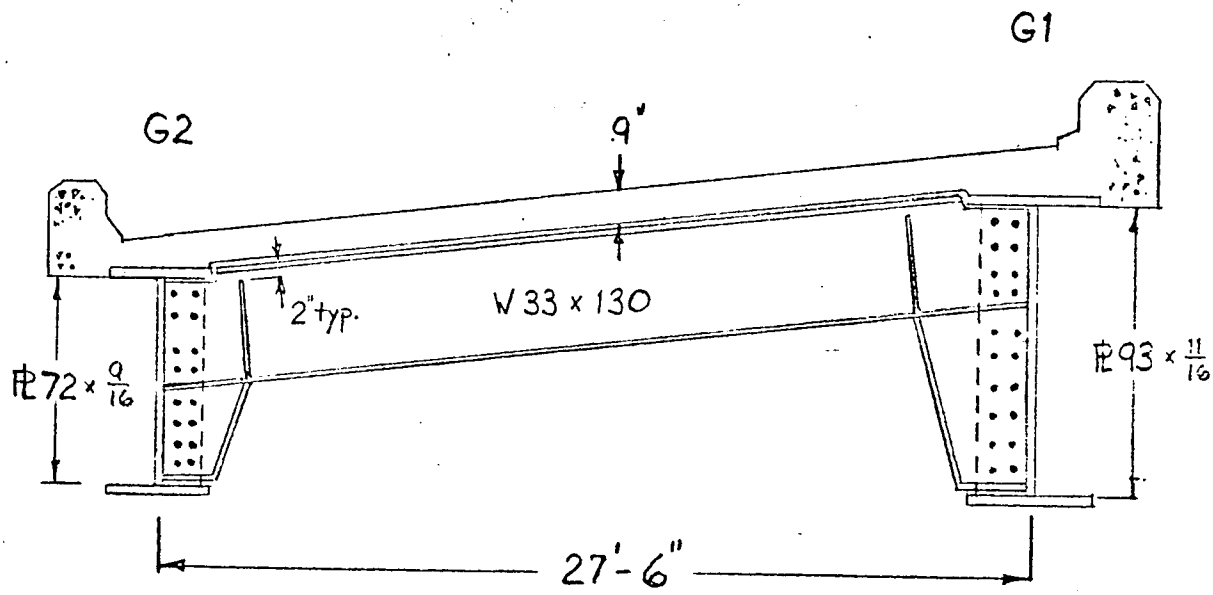

Typical Cross Section

Figure 4

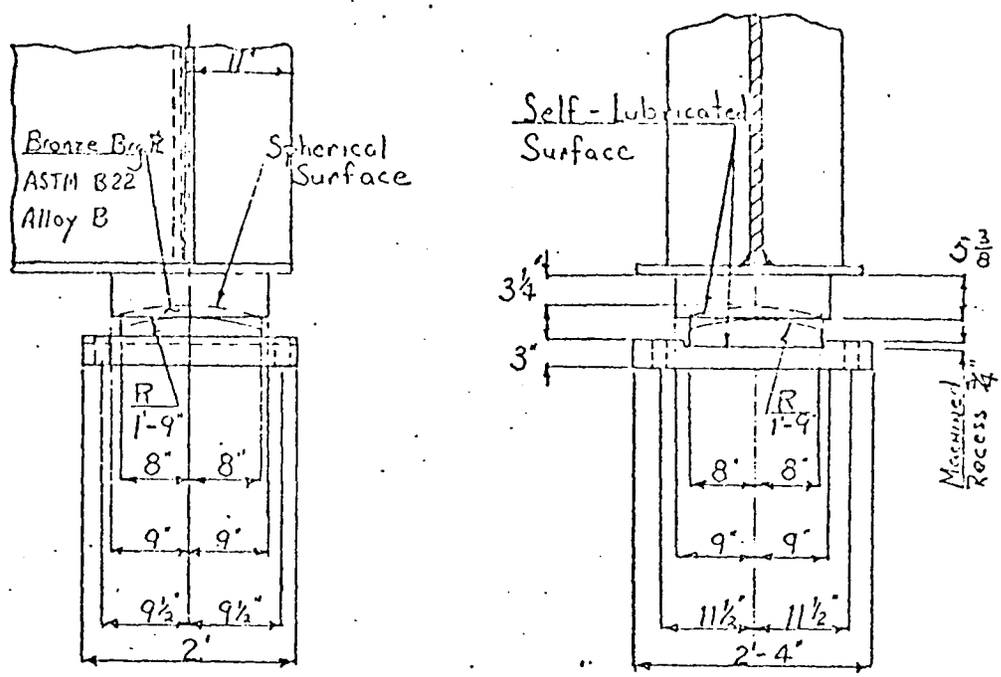

Expansion Shoe - G1

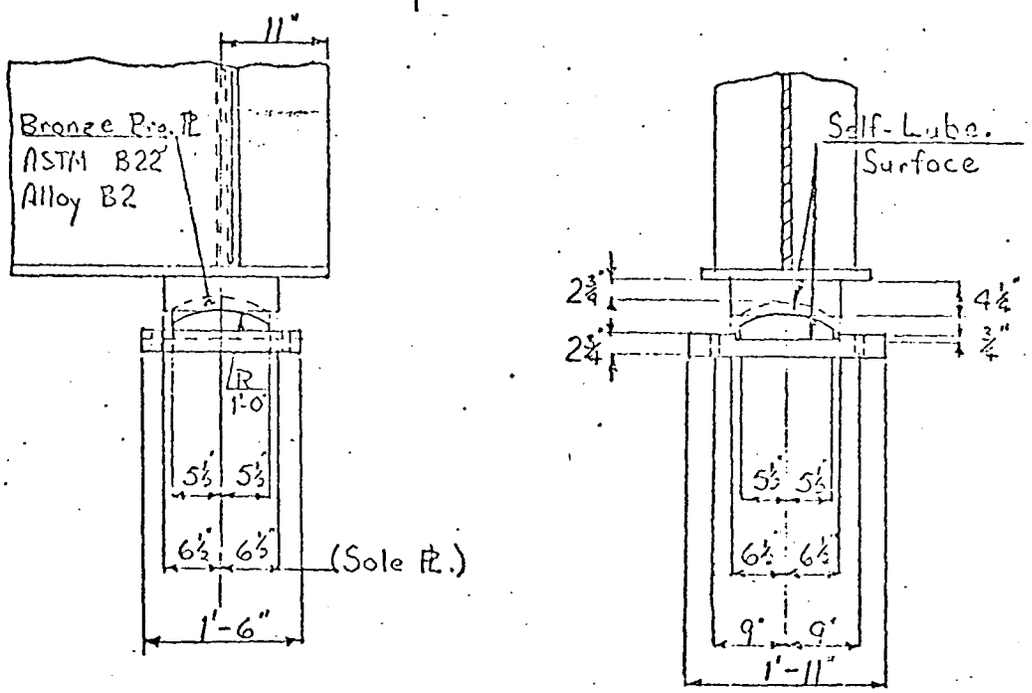

Expansion Shoe - G2

Figure - 5a

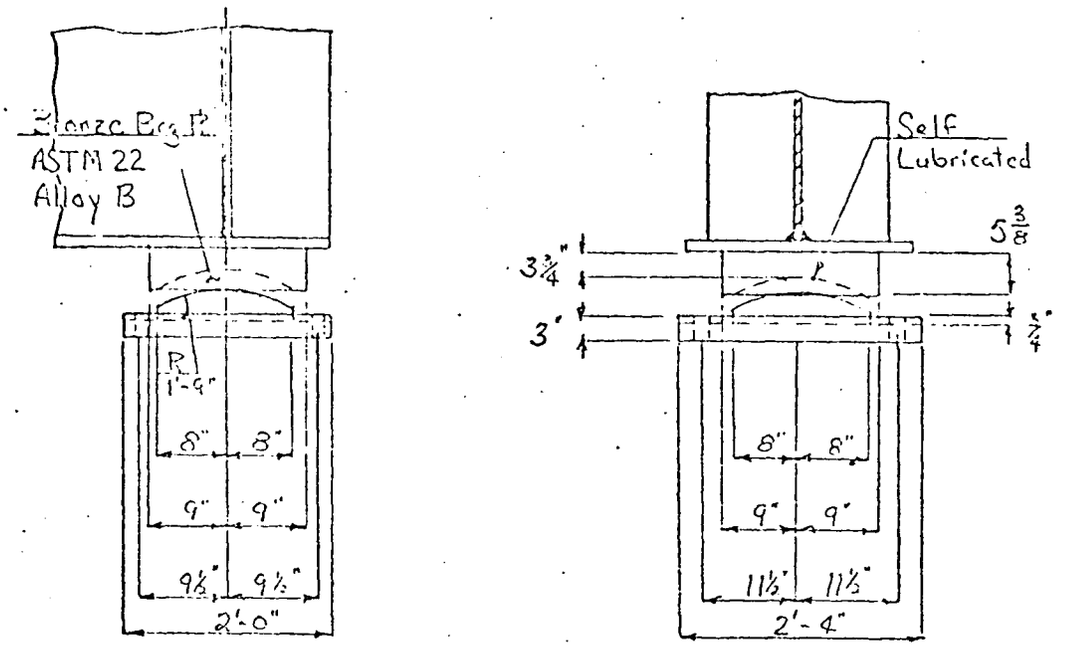

Fixed Shoe - G1

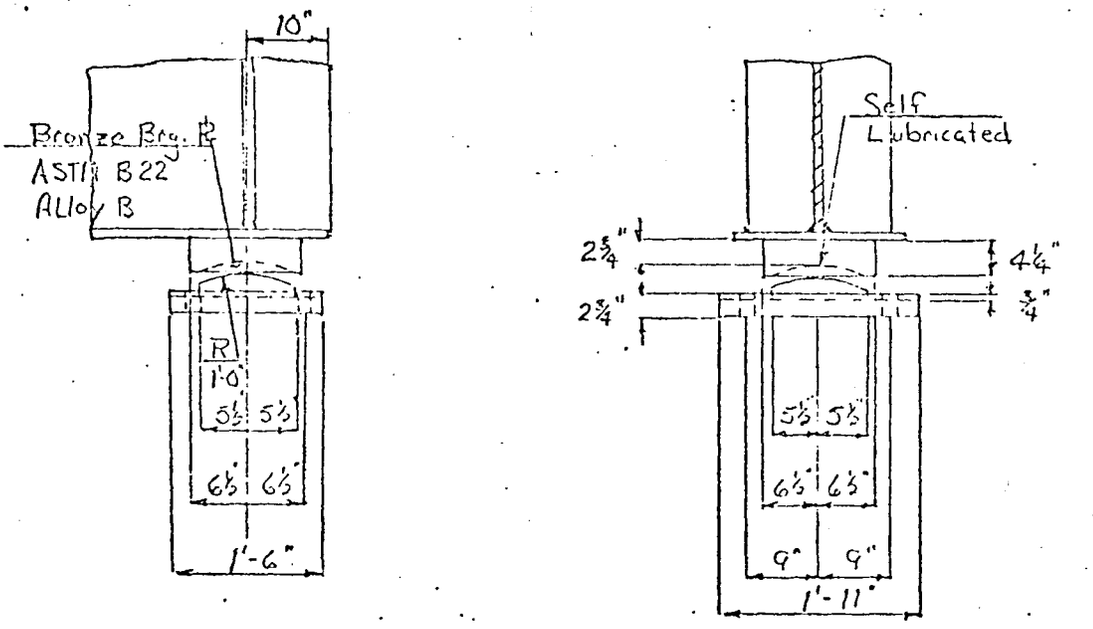

Fixed Shoe - G2

Figure 5b

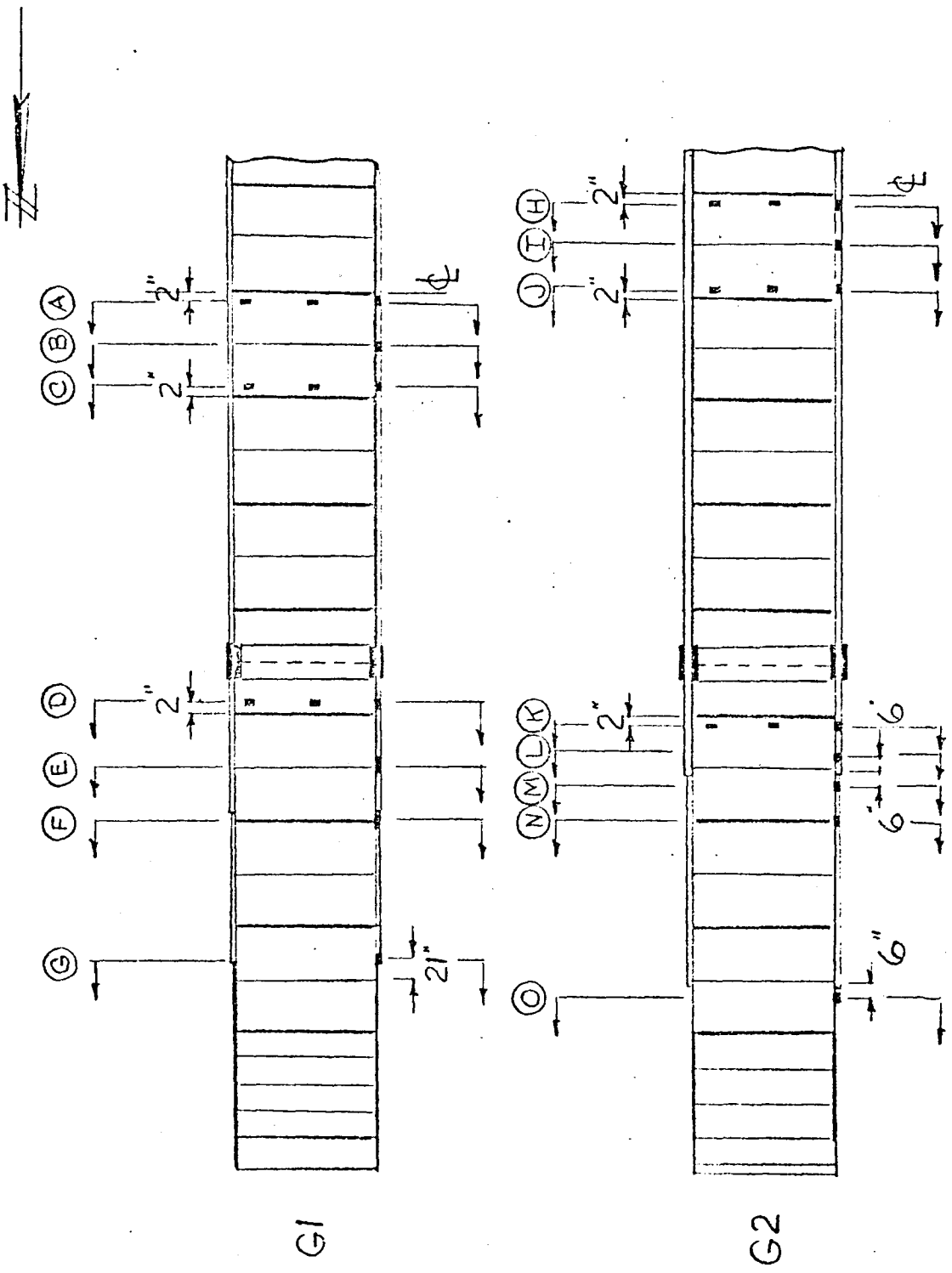

Figure 6 - Strain gage locations

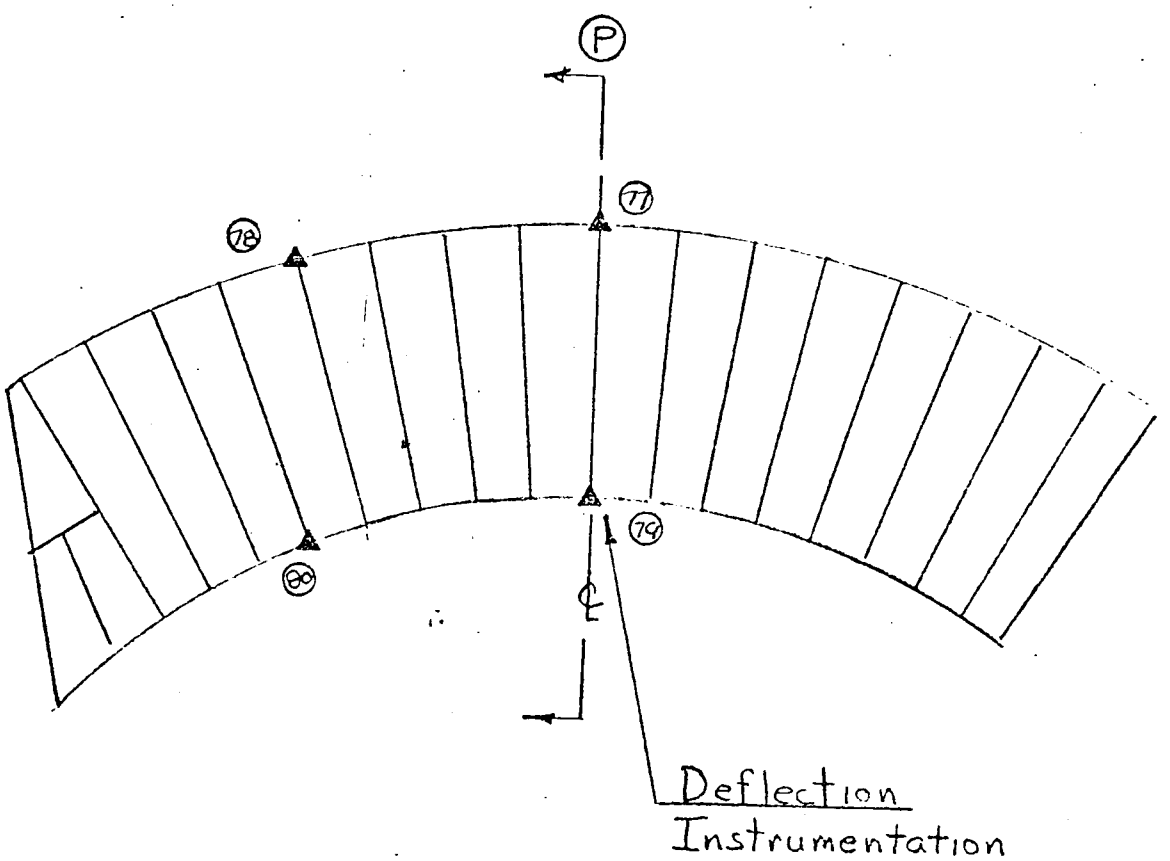

Figure 7- Gage Locations

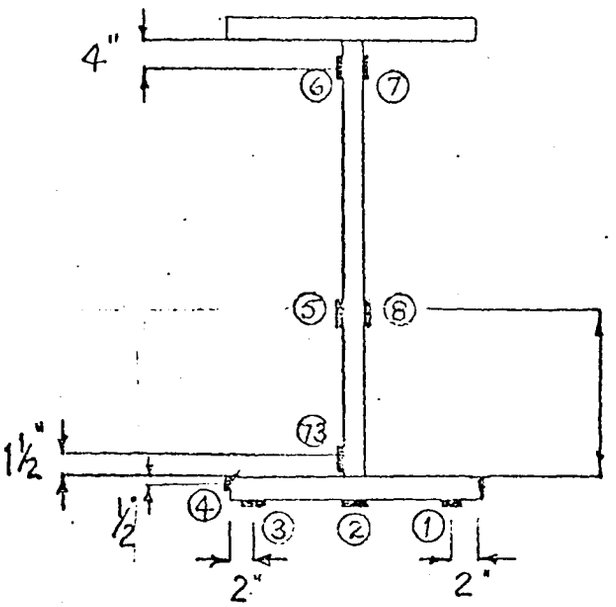

Section A

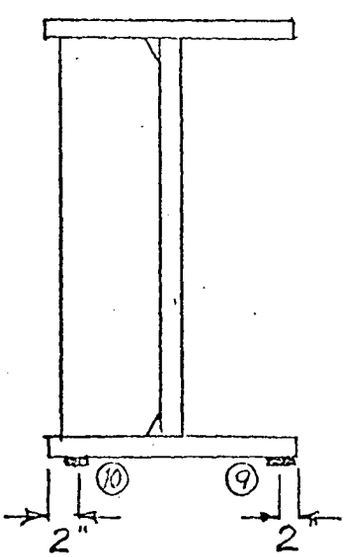

Section B

Figure 8 - Gage Locations ; G1

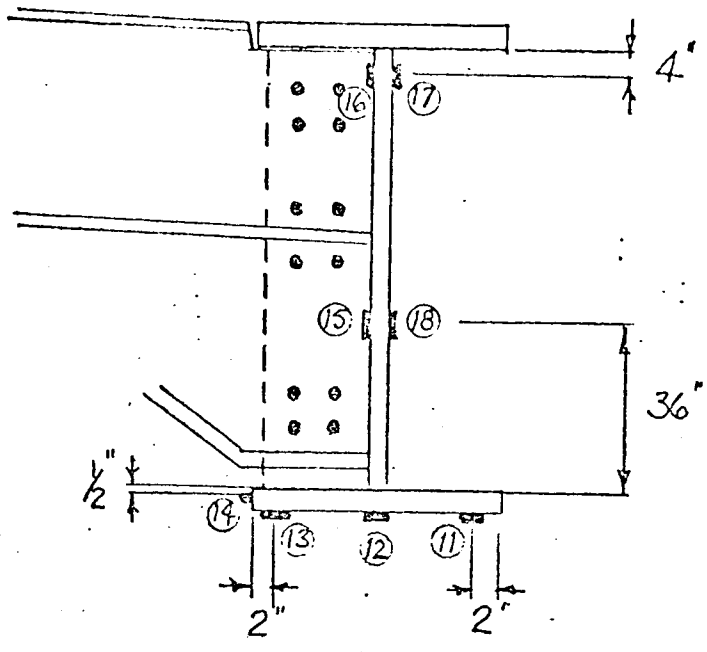

Section C

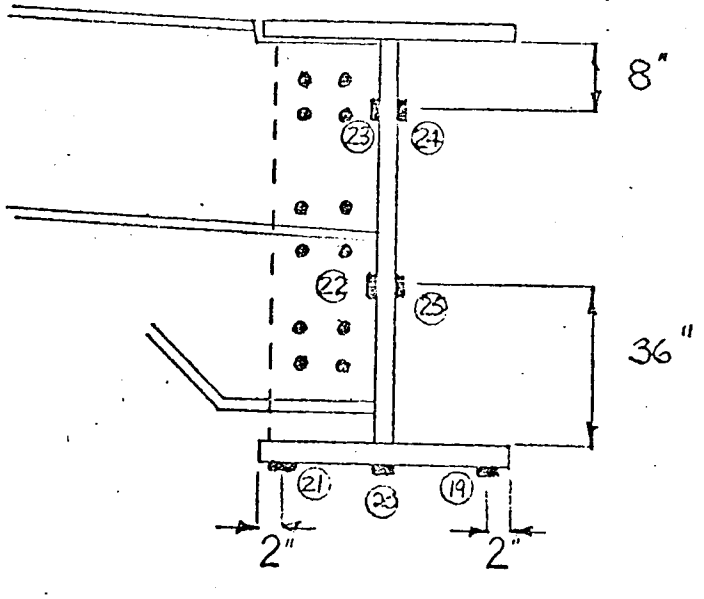

Section D

Figure 9 - Gage Locations ; G1

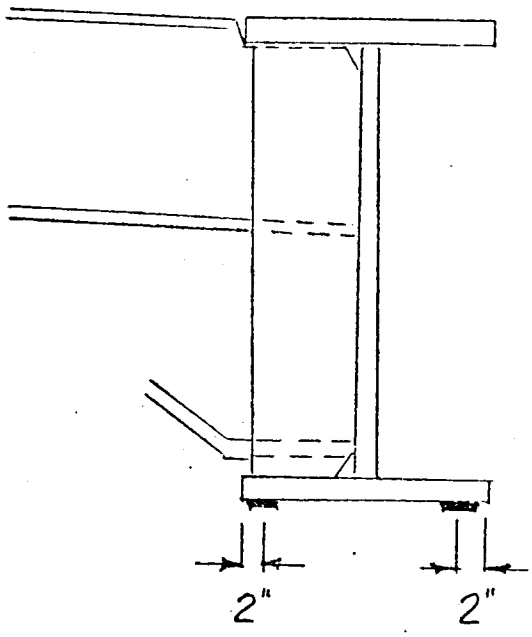

Figure 10 - Gage Locations ; G1

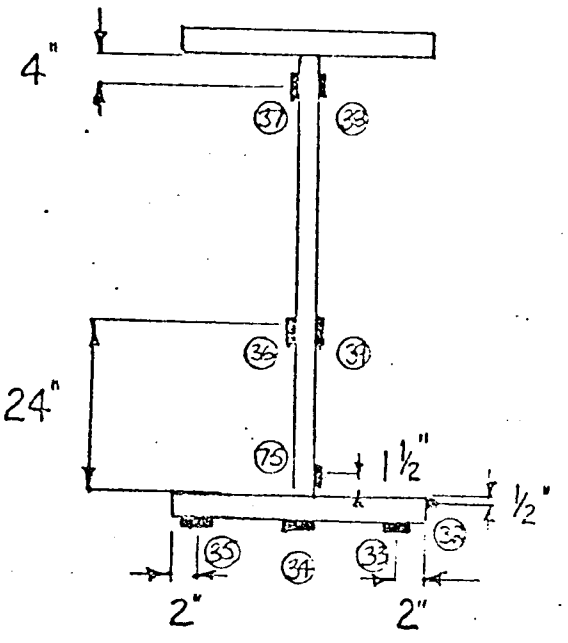

Section H

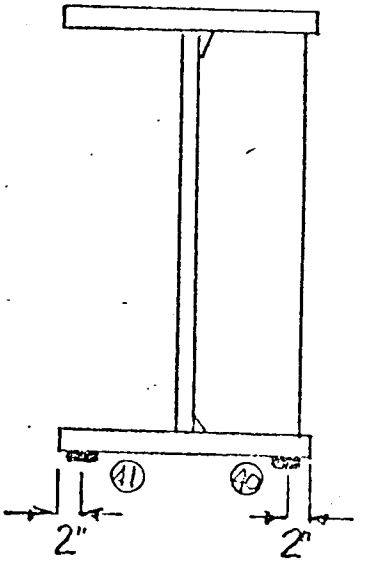

Section I

Figure 11 - Gage Locations ; G2

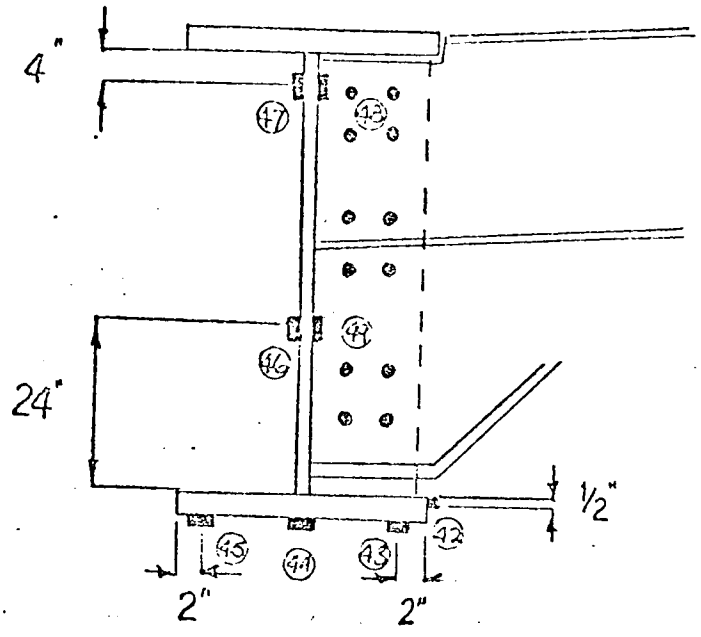

Section J

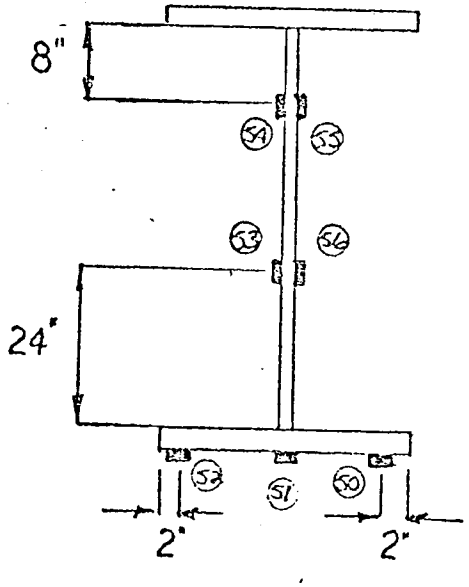

Section K

Figure 12- Gage Locations ; G2

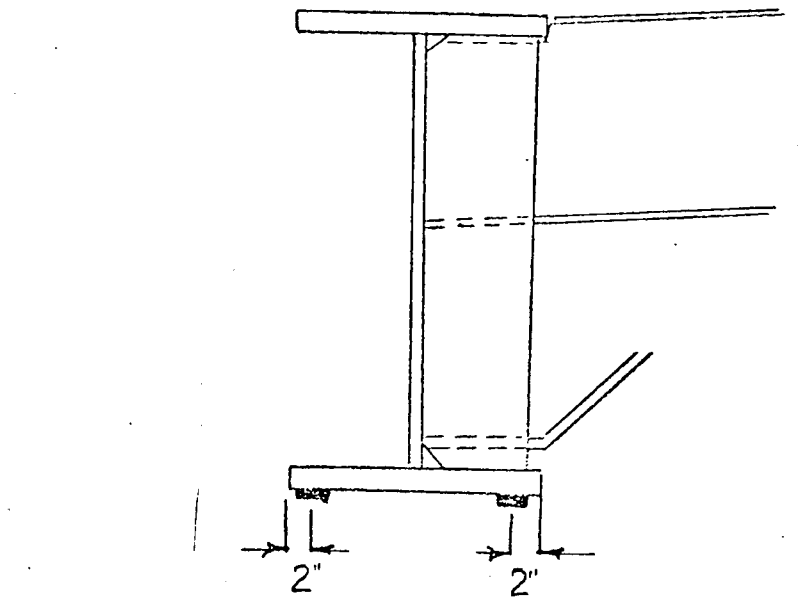

Section L	58	57
Section M	60	59
Section N	62	61
Section O	64	63

Figure 13 - Gage Locations ; G2

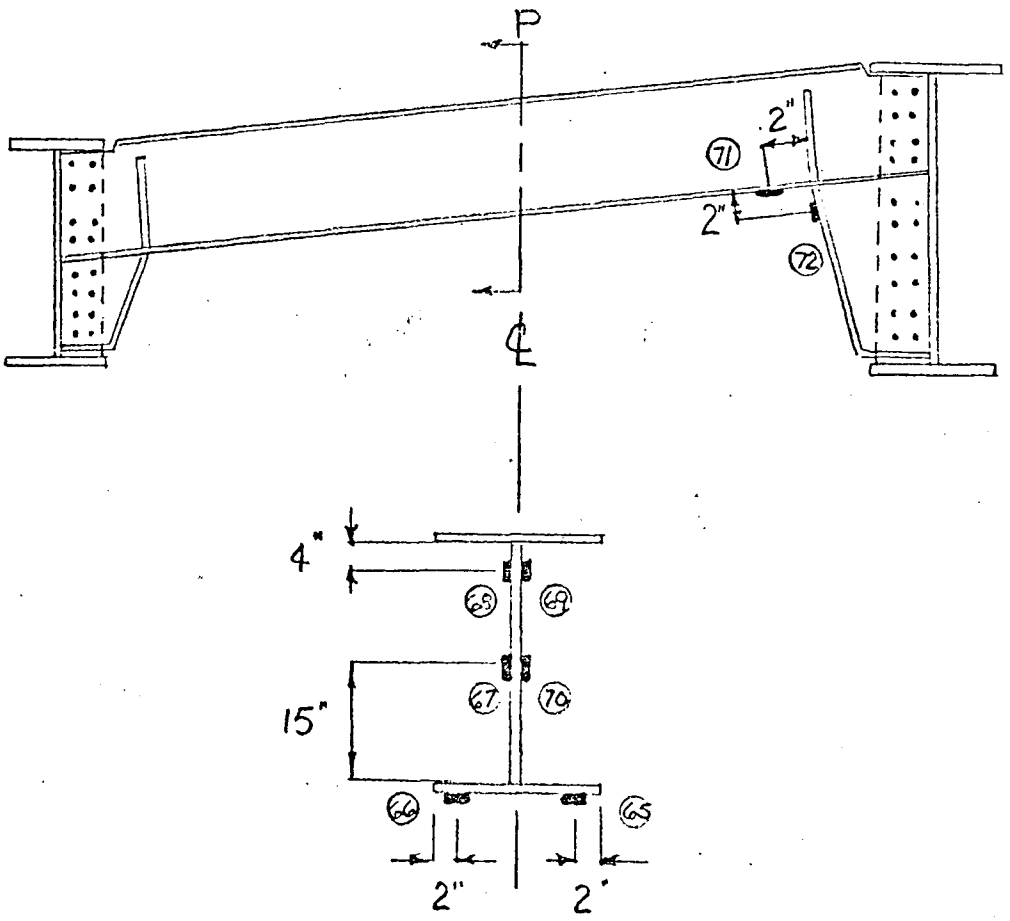

Section P

Figure 14 - Gage Locations - Cross Bracing

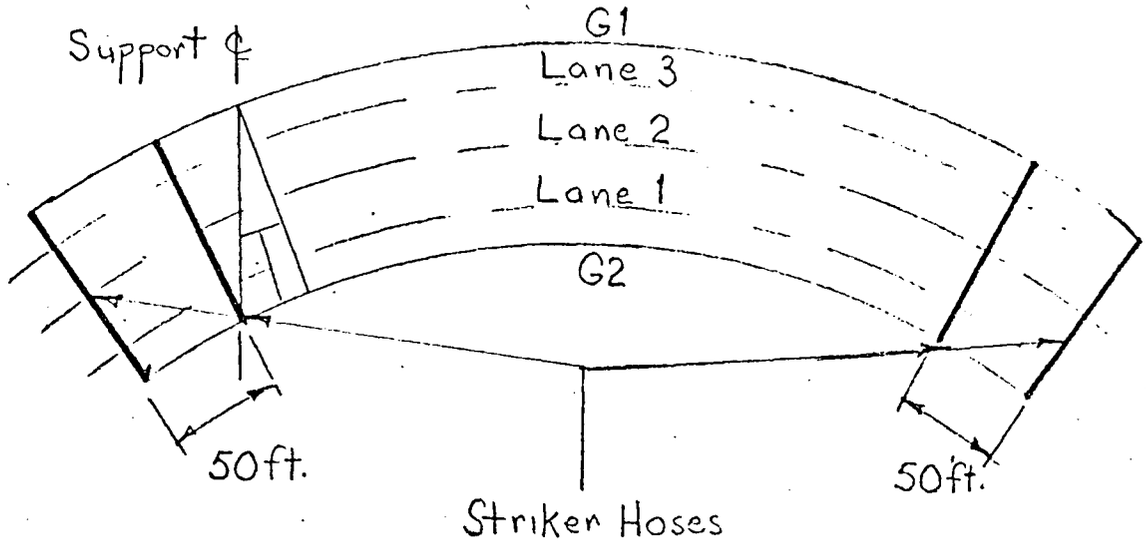

Plan View

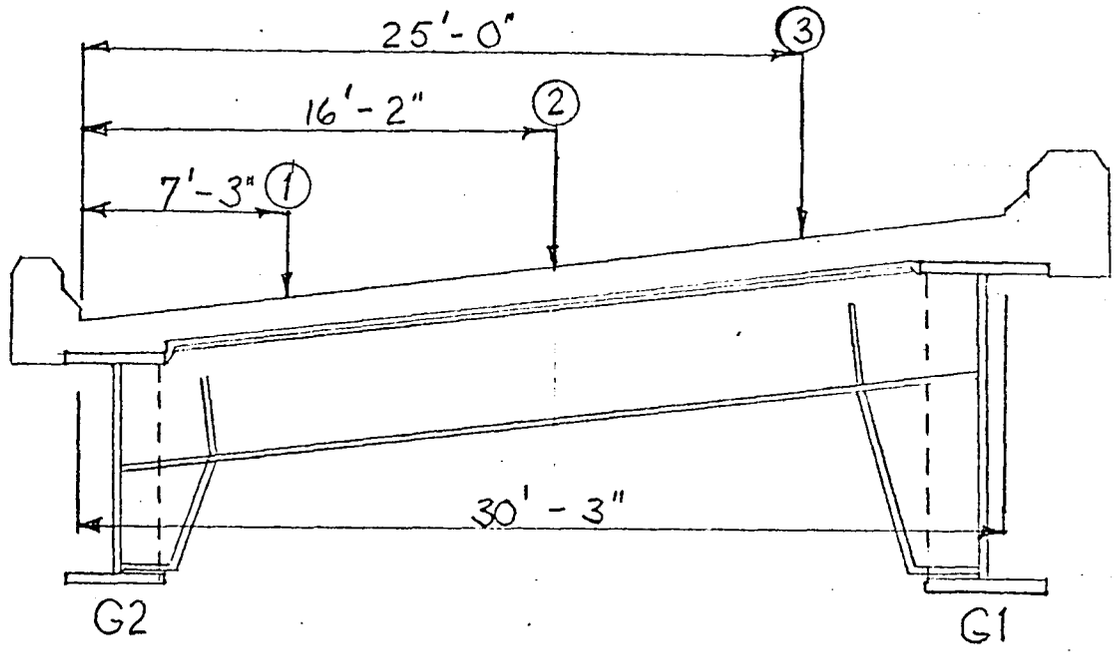

Figure 15 - Deck Layout

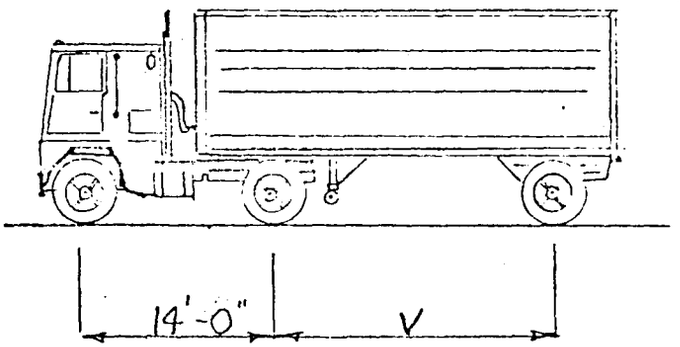

Axle Loads - 8 kips 32 kips 32 kips = 72 kips

AASHTO Truck Load - HS 20-44

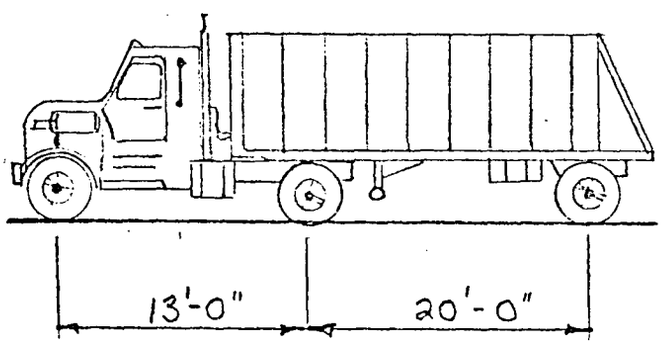

Axle Loads - 10.12 kips 35.42 kips 32.84 kips = 78.38 kips

FHWA Test Truck - HS 20-44

Figure 16 - Truck Loads

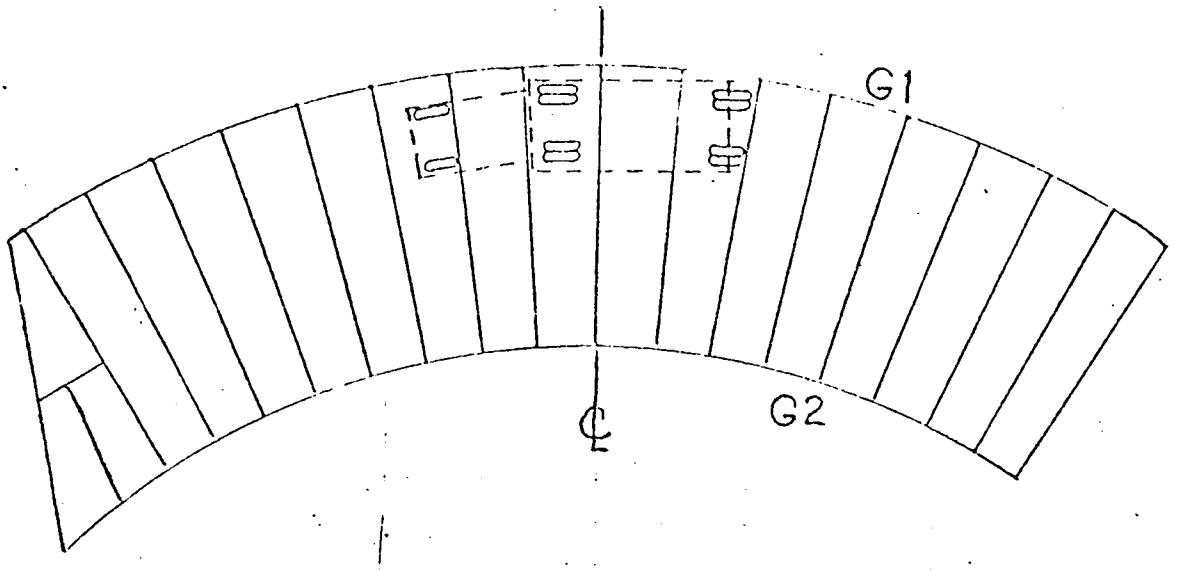

Load Case 1 - Lane 3

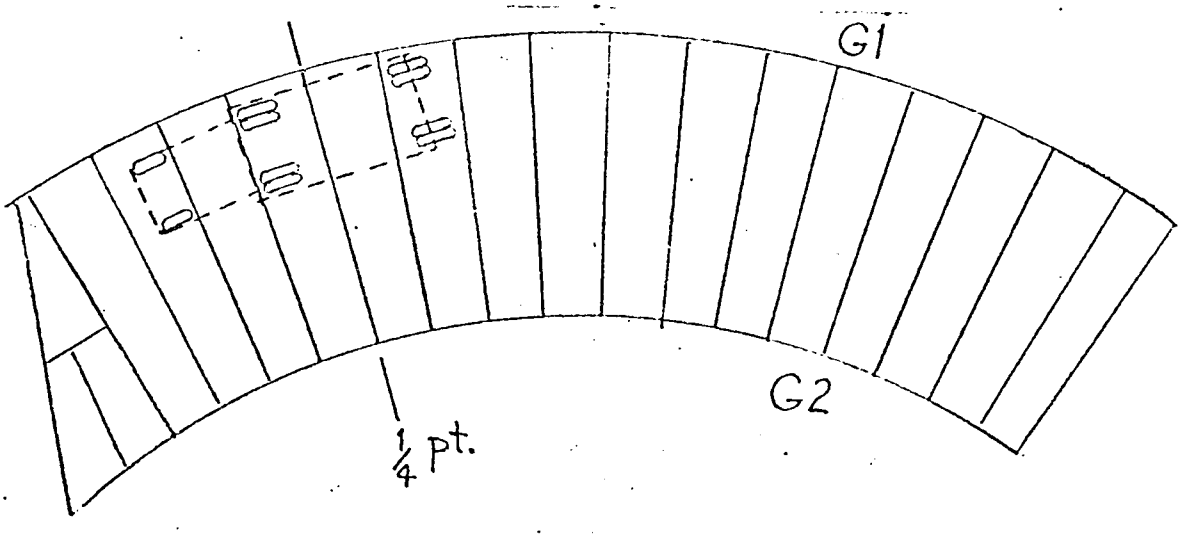

Load Case 2 - Lane 3

Figure 17a - Static Load Positions

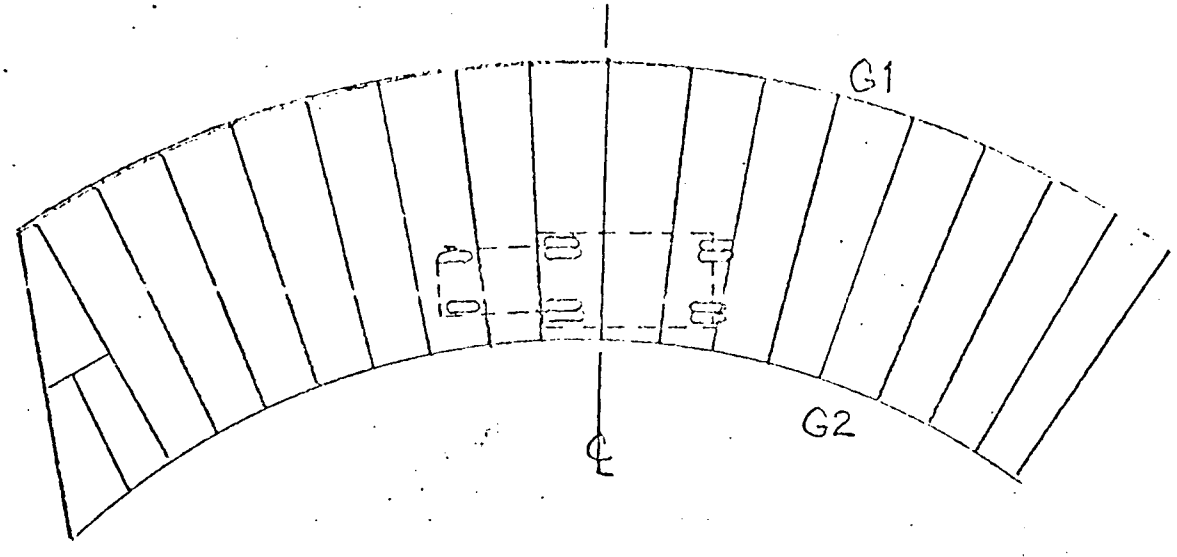

Load Case 4- Lane 1

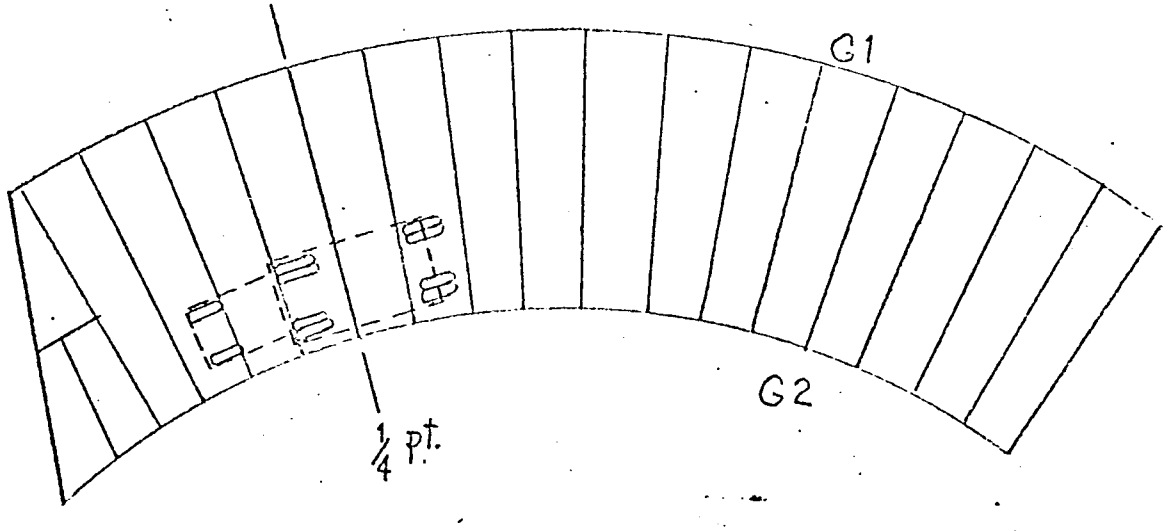

Load Case 3 - Lane 1

Figure 17b Static Load Positions

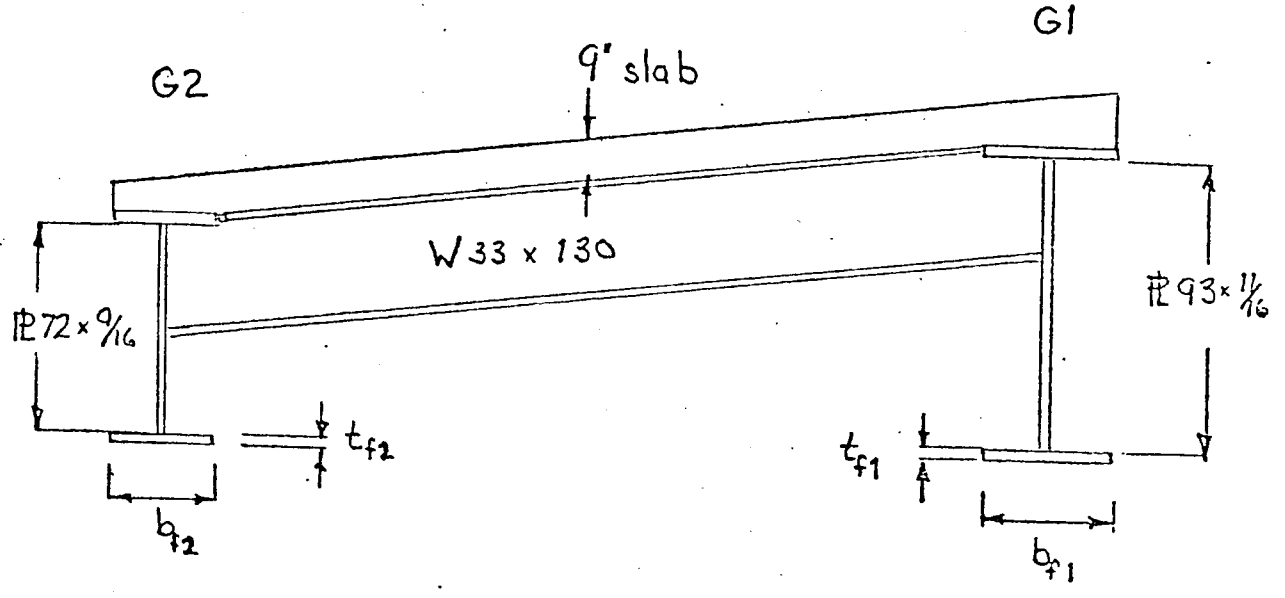

Note: 1. Flange thickness and width varies as specified along span.

2. Composite action is assumed

Figure 18 CURVBRG Cross Section

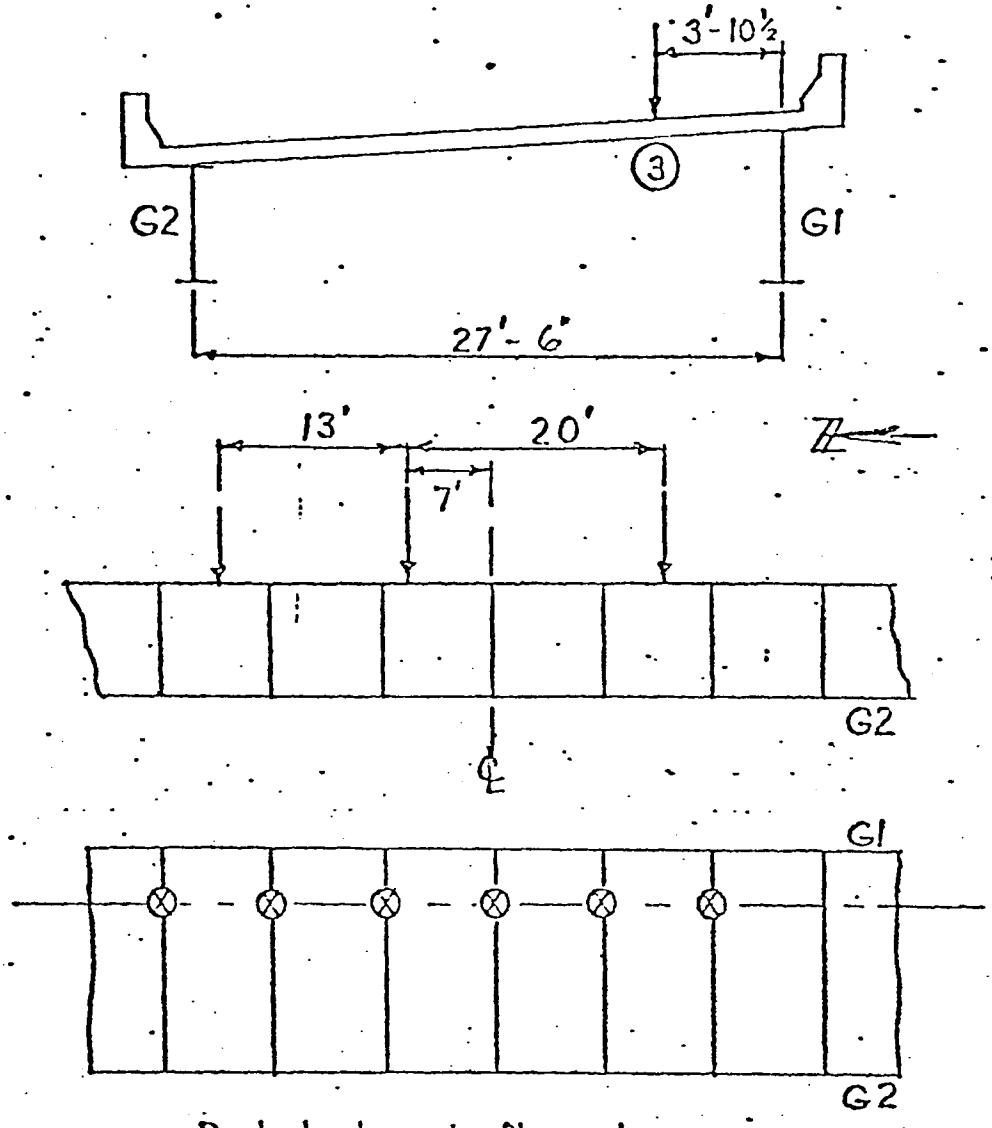

Figure 19 – CURVBRG Load Scheme
Load Case 1

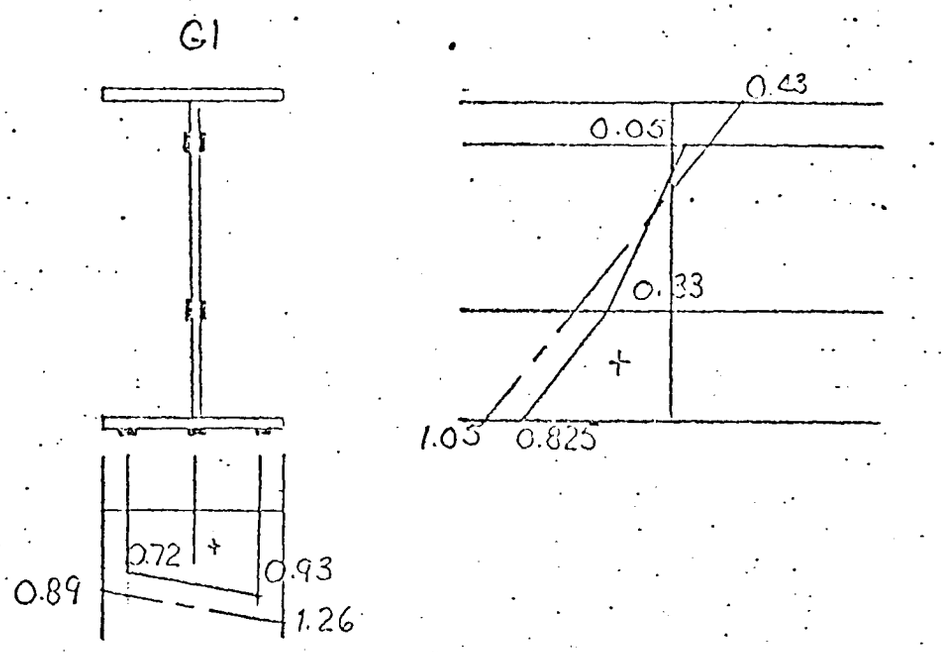

Section A

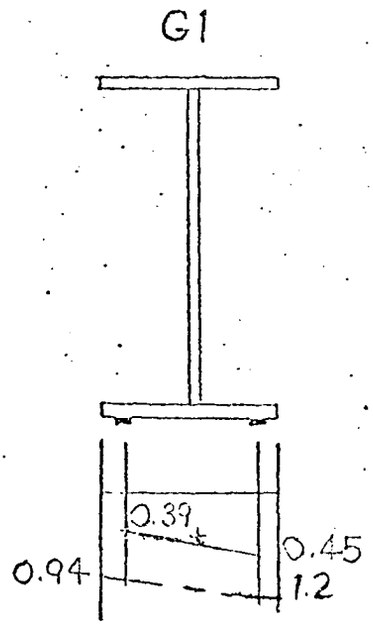

Section B

Figure 20 Stress Diagrams - Load Case 4

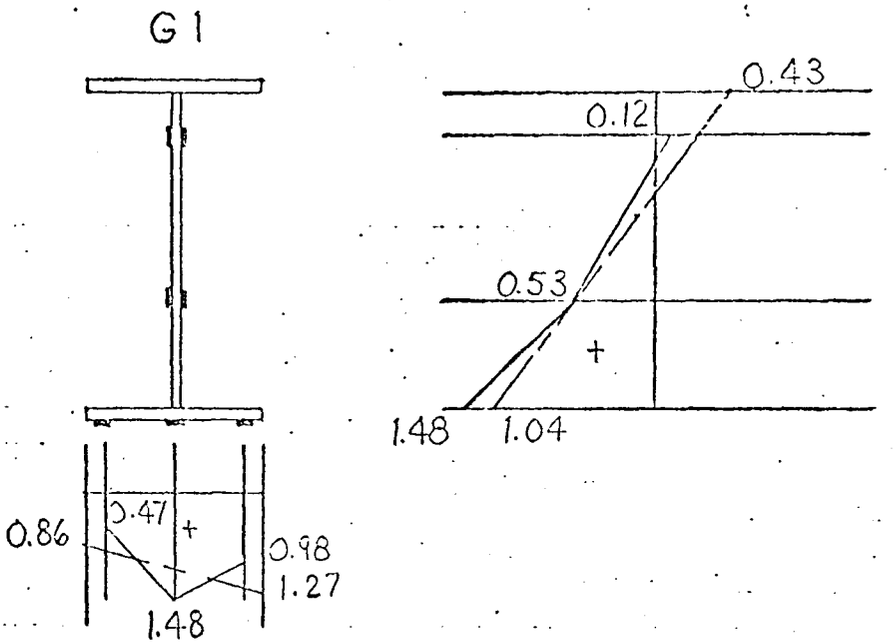

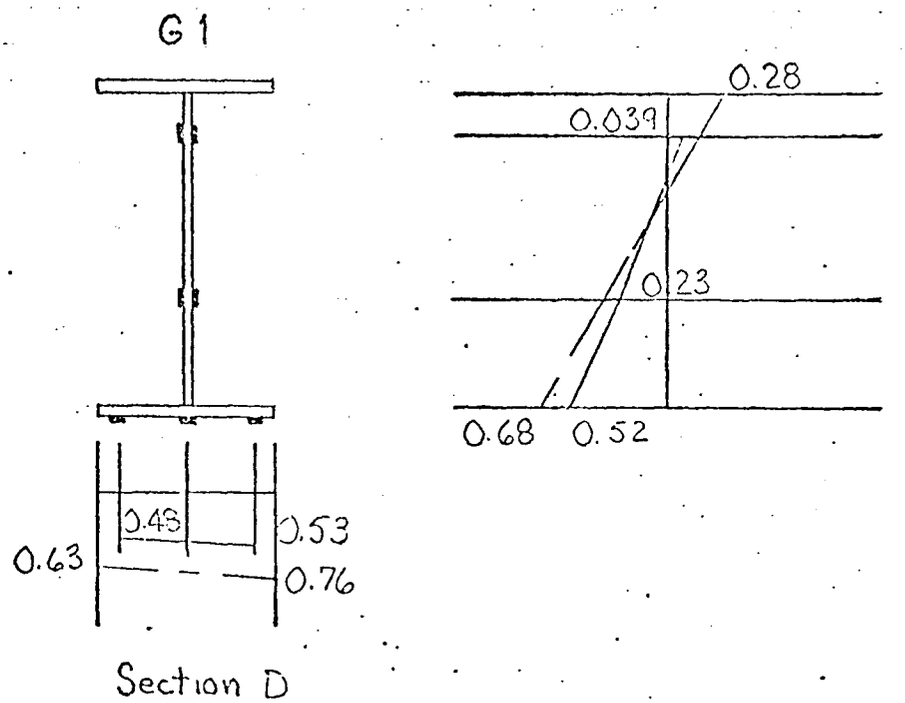

Figure 21 Stress Diagrams - Load Case 4

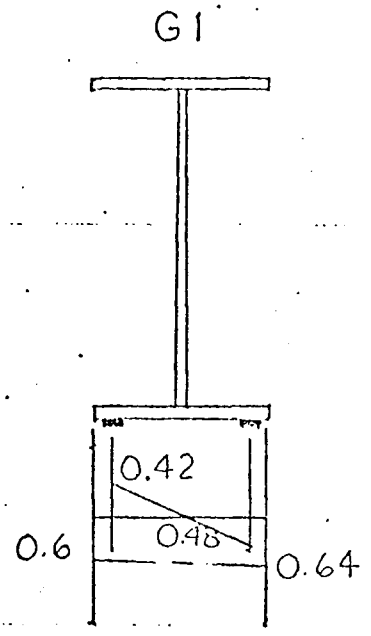

Section E

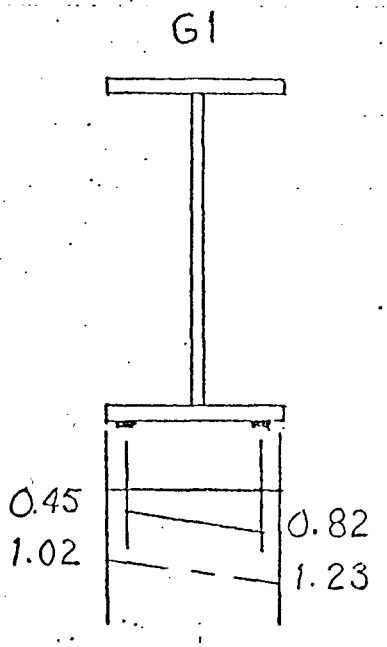

Section F

Figure 22 Stress Diagrams - Load Case 4

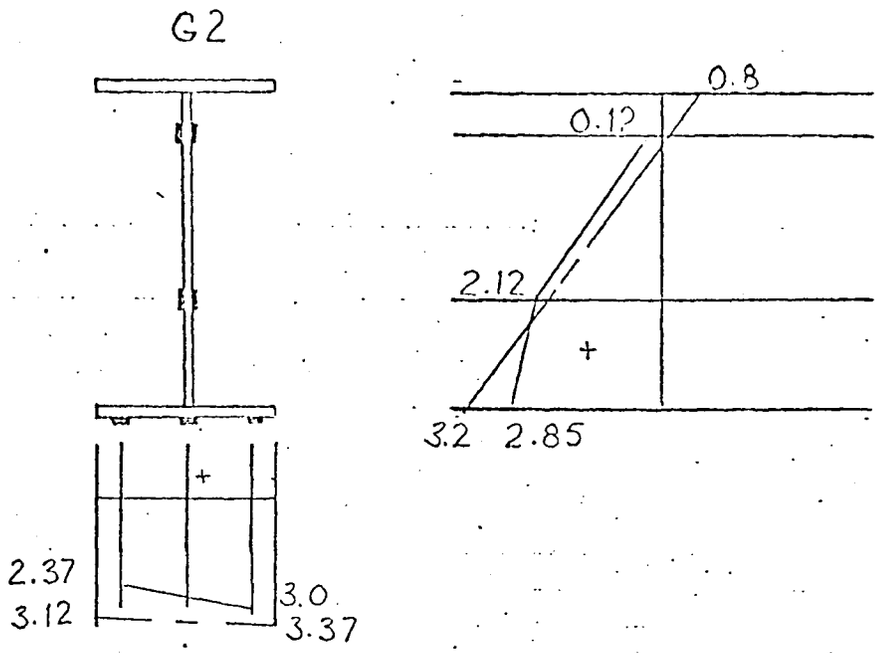

Figure 23 Stress Diagrams - Load Case 4

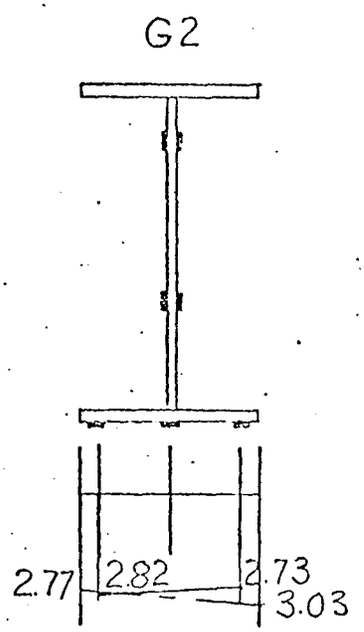

Section J

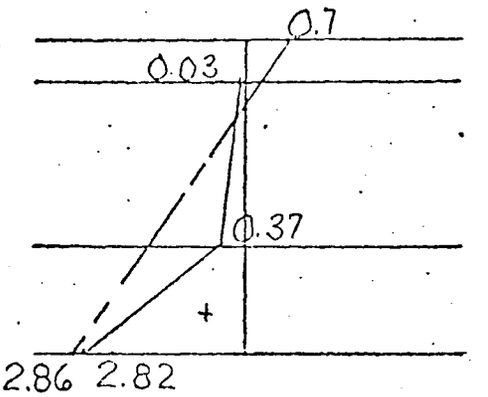

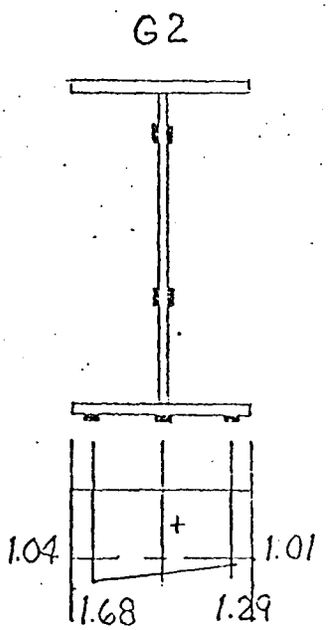

Section K

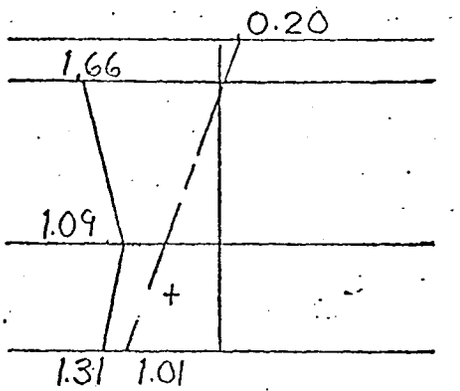

Figure 24 Stress Diagrams - Load Case 4

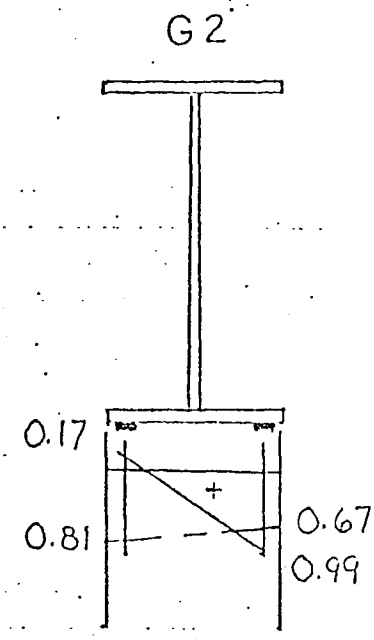

Section L

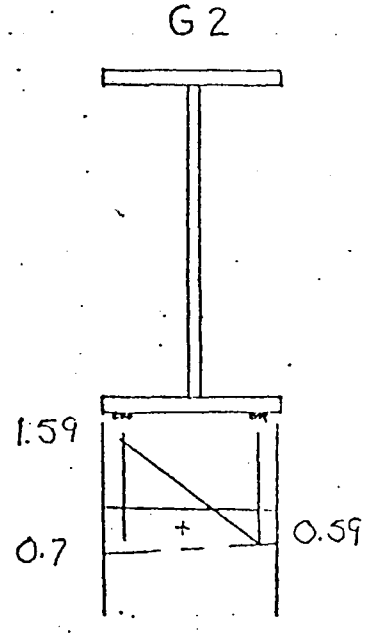

Section M

Figure 25 Stress Diagrams - Load Case 4

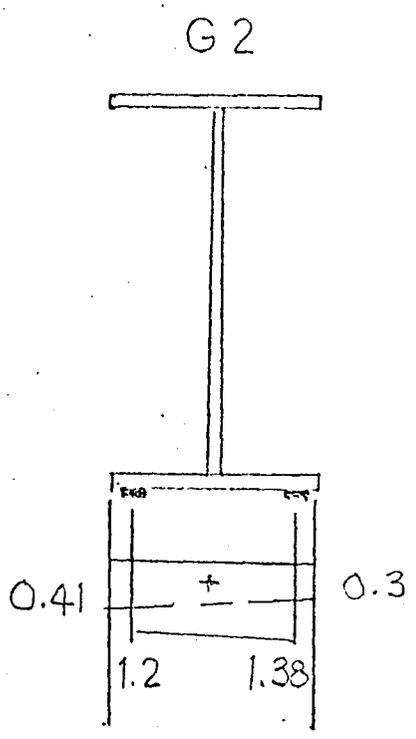

Section N

Figure 26 Stress Diagram - Load Case 4

Run No. 11 - Northbound

Speed = 33.76 mph

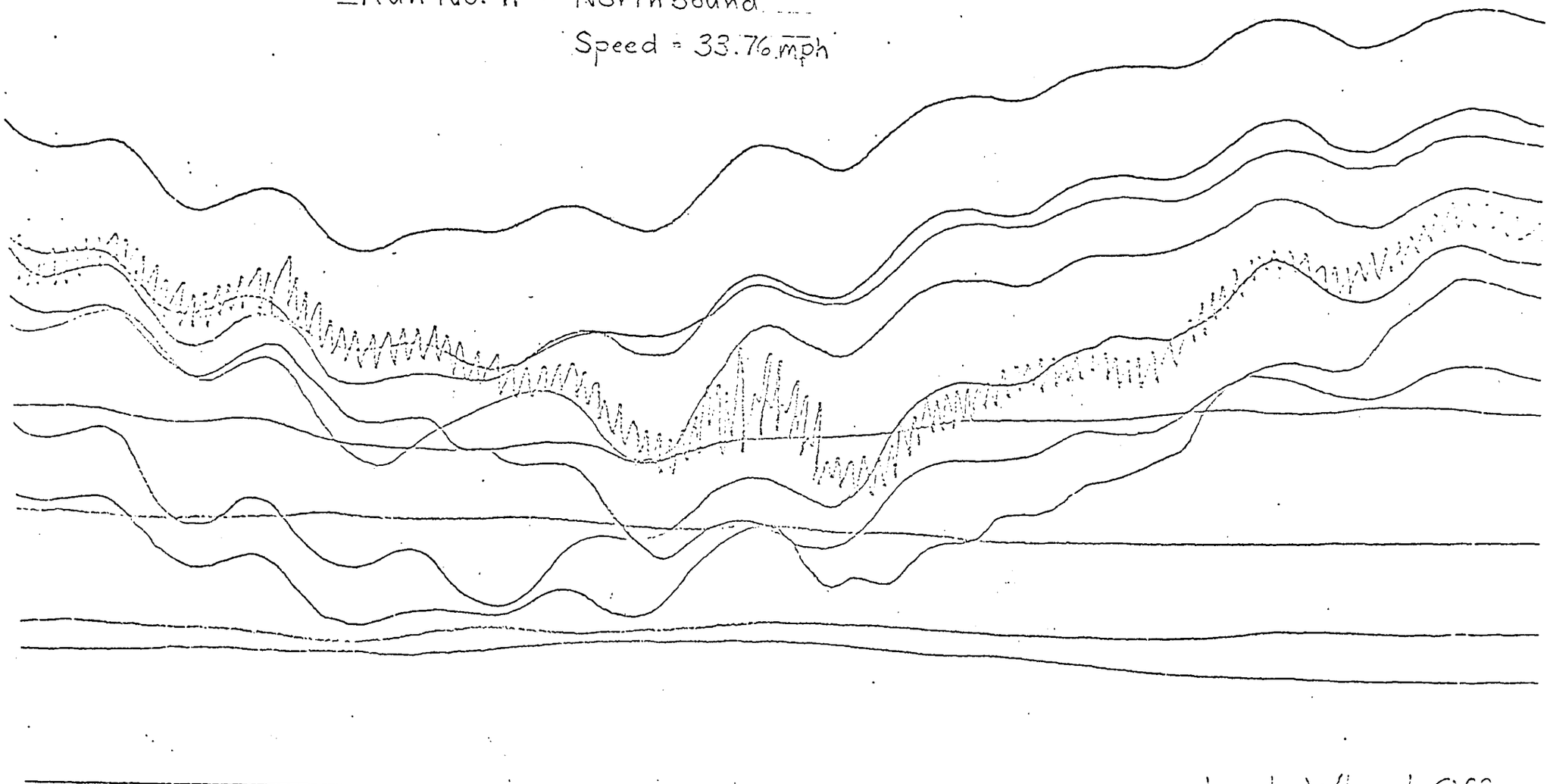

Figure 27 - Analog Trace Recording

REFERENCES

1. Culver, C.G. and Mozer, J.D.
   PART 1: SUMMARY REPORT, CHAPTER 8 - STABILITY, Excert from Curt Final Report, Carnegie - Mellon University, (May 1973).

2. Armstrong, W.L. and Greig, R.A.
   BEHAVIOR OF A CURVED STEEL BOX BEAM BRIDGE, Public Roads, Vol. 37, No. 7, p. 262, (Dec. 1973).

3. Armstrong, W.L.
   DYNAMIC TESTING OF CURVED BRIDGE-HUYCK STREAM, Journal of the Structural Division, ASCE, Vol. 98, No. St. 9, p. 2015, (Sept. 1972).

4. Powell, G.H.
   CURVBRG: A COMPUTER PROGRAM FOR ANALYSIS OF CURVED OPEN GIRDER BRIDGES, University of California at Berkeley, (May 1973).

5. Marchica, N.V., Yen, B.T. and Fisher, J.W.
   STRESS HISTORY STUDY OF THE ALLEGHENY BRIDGE (PENNSYLVANIA TURNPIKE), Fritz Engineering Laboratory, Report No. 386.3, Lehigh University, (May 1974).

6. STANDARD SPECIFICATIONS FOR HIGHWAY BRIDGES, Tenth Edition, American Association of State Highway Officials, Washington, D.C. 1969.

7. ANALYSIS AND DESIGN OF HORIZONTALLY CURVED STEEL BRIDGE GIRDERS, United States Steel Structural Report ADUCO 91063, (May 1963).

8. Fisher, J.W.
   GUIDE TO 1974 AASHTO FATIGUE SPECIFICATIONS, American Institute of Steel Construction, (May 1974).

ACKNOWLEDGEMENT

The bridge described in this paper was tested in conjunction with the Pennsylvania Department of Transportation (PennDOT) and the Federal Highway Administration (FHWA) under project 398 "Fatigue Strength of Curved Steel Bridge Elements" currently underway at Fritz Engineering Laboratory, Lehigh University. Dr. Lynn S. Beedle is the Director of the laboratory and Dr. David A. VanHorn is the Chairman of the Department of Civil Engineering.

Special thanks are given to Dr. Ben T. Yen, Associate Professor of Civil Engineering at Lehigh University, for his supervision and untiring efforts during the writing of this thesis. Also, to Dr. J. Hartley Daniels, Associate Professor of Civil Engineering at Lehigh University, for the opportunity to assist on Project 398.

In addition, special thanks are extended to Debbie Zappasodi and Antoinette Larkin for their expertise in typing the manuscript.

VITA

John M. Talhelm, the son of Margaret and John J. Talhelm, was born on May 9, 1950 in Binghamton, New York. The author attended Catholic Central High School in Binghamton where he graduated with honors. He was a Dean's List student at Manhattan College in the Bronx, New York where he received a Bachelor of Engineering Degree in Civil Engineering in June, 1973. He was awarded a Research assistantship in Civil Engineering at Fritz Engineering Laboratory, Lehigh University in October, 1973 and received his Master of Science Degree in Civil Engineering from Lehigh University in May, 1975.